Heat transfer analysis in the flow of Walters' B fluid with a convective boundary condition*

T. Hayat[a)b)], Sadia Asad[a)†], M. Mustafa[c)], and Hamed H. Alsulami[b)]

[a)] *Department of Mathematics, Quaid-i-Azam University* 45320, *Islamabad* 44000, *Pakistan*
[b)] *Department of Mathematics, Faculty of Science, King Abdulaziz University, Jeddah* 21589, *Saudi Arabia*
[c)] *School of Natural Sciences, National University of Science and Technology (NUST), Sector H*-12, *Islamabad* 44000, *Pakistan*

(Received 10 October 2013; revised manuscript received 16 December 2013; published online 20 June 2014)

Radiative heat transfer in the steady two-dimensional flow of Walters' B fluid with a non-uniform heat source/sink is investigated. An incompressible fluid is bounded by a stretching porous surface. The convective boundary condition is used for the thermal boundary layer problem. The relevant equations are first simplified under usual boundary layer assumptions and then transformed into a similar form by suitable transformations. Explicit series solutions of velocity and temperature are derived by the homotopy analysis method (HAM). The dimensionless velocity and temperature gradients at the wall are calculated and discussed.

Keywords: Walters' B fluid, heat source/sink, convective boundary condition, analytic solution

PACS: 47.15.Cb, 47.50.−d **DOI:** 10.1088/1674-1056/23/8/084701

1. Introduction

Non-Newtonian fluid flows have gained significant importance in the last decade because of their diverse applications in various disciplines. The Walters' B fluid model can describe the behaviors of various polymeric liquids encountered in biotechnology and chemical engineering. Beard and Walter[1] discussed the elastico-viscous boundary layer flow near a stagnation point. They proposed the constitutive equations for elastico-viscous fluids formally known as Walters' B liquids. The flow of an elastico-viscous fluid past an infinite impermeable plate moving impulsively in its own plane was studied by Soundalgekar.[2] Sapria *et al.*[3] investigated the flow of an electrically conducting incompressible elastico-viscous fluid filling a semi-infinite plate in contact with an infinite non-conducting plate. Two-dimensional (2D) flow of Walters' B fluid over a stretching sheet was studied by Rajagopal *et al.*[4] The regular perturbation method was employed to yield a solution for small values of viscoelastic parameters. The resulting zeroth and first order differential systems were solved numerically by the Runge–Kutta integration technique. Labropulu *et al.*[5] examined the effect of a slip boundary condition on the stagnation-point flow of Walters' B fluid. Khan and Sanjayanand[6] discussed the flow of elastico-viscous fluid past an exponentially stretching sheet. Cortell[7] studied the 2D boundary layer flow of second grade and Walters' B fluid over a stretching sheet with mass transfer. Abel *et al.*[8] studied the MHD flow and heat transfer of elastico-viscous fluid over a stretching sheet with Ohmic heating and viscous dissipation. Hayat *et al.*[9] provided homotopy solutions for a three-dimensional (3D) flow of elastico-viscous fluid. In another paper, Hayat *et al.*[10] discussed the mass transfer effects in the (3D) MHD flow of viscoelastic fluid bounded by a stretching sheet. Few representative studies of non-Newtonian fluids may be mentioned through Refs. [11]–[18].

Heat transfer with convective boundary conditions has obvious importance in thermal energy storage, gas turbines, nuclear turbines, die forging, and chemical reaction. Similarity solutions for the laminar flow over a flat plate (the so-called Blasius flow) with convective boundary condition were obtained by Aziz.[19] He used the fourth–fifth order Runge–Kutta method with a shooting technique for the numerical solution. An exact solution to the problem considered in Ref. [19] was obtained by Magyari.[20] Mixed convection stagnation point flow of non-Newtonian fluid over a stretching sheet with convective boundary conditions has been investigated by Hayat *et al.*[21] Ishak[22] provided the numerical solution for the flow and heat transfer over a permeable stretching sheet with convective boundary conditions. A closed form exact solution for the fundamental stretching/shrinking wall problem in the presence of convective boundary conditions has been computed by Yao *et al.*[23] Hayat *et al.*[24,25] obtained homotopy solutions for the flow of Jeffrey and second grade fluids respectively with convective boundary conditions. Mustafa *et al.*[26] recently explored the axisymmetric flow of nanofluid over a radially stretching sheet with convective boundary conditions. Moreover, the recent heat conduction problems have been investigated by Jianfei and Yumin,[27] Li *et al.*[28] and Zhang *et al.*[29]

To the best of our knowledge, there is not a single ar-

*Projects supported (for Alsulami) by Deanship of 13 Scientific Research (DSR), King Abdulaziz University, Jeddah, Saudi Arabia.
†Corresponding author. E-mail: asadsadia@ymail.com
© 2014 Chinese Physical Society and IOP Publishing Ltd

ticle that addresses the effect of heat transfer in an elastico-viscous boundary layer flow with a convective boundary condition. Therefore, the present work addresses this concept in the presence of a non-uniform heat source/sink. The relevant equations are first modeled and then solved by a modern technique namely the homotopy analysis method (HAM).[30–39] The dimensionless expressions of the wall shear stress and the local heat transfer rate at the wall are calculated and discussed.

2. Problem formulation

We consider the steady and 2D flow of an incompressible Walters' B fluid over a porous surface. In addition, heat transfer analysis is considered with radiation effects and non-uniform heat source/sink. Further, we consider the x axis parallel to the sheet and the y axis normal to it. The extra stress tensor $\boldsymbol{S}$ for Walters' B fluid is defined by

$$\boldsymbol{S} = 2\eta_0 \boldsymbol{A}_1 - 2k_0 \frac{\mathrm{d}\boldsymbol{A}_1}{\mathrm{d}t}, \tag{1}$$

$$\frac{\mathrm{d}\boldsymbol{A}_1}{\mathrm{d}t} = \frac{\partial \boldsymbol{A}_1}{\partial t} + \boldsymbol{V}\cdot\boldsymbol{\nabla}\boldsymbol{A}_1 - \boldsymbol{A}_1\cdot\boldsymbol{\nabla}\boldsymbol{V} - (\boldsymbol{\nabla}\boldsymbol{V})^{\mathrm{T}}\cdot\boldsymbol{A}_1, \tag{2}$$

where $\boldsymbol{A}_1$ is the rate of strain tensor, $\boldsymbol{V}$ is the velocity field of fluid, $\mathrm{d}\boldsymbol{A}_1/\mathrm{d}t$ is the covariant derivative of the rate of strain tensor in relation to the material in motion, and η_0 and k_0 are the limiting viscosity at small shear rate and short memory coefficient respectively. These are defined as follows:

$$\eta_0 = \int_0^\infty N(\tau)\mathrm{d}\tau, \tag{3}$$

$$k_0 = \int_0^\infty \tau N(\tau)\mathrm{d}\tau, \tag{4}$$

with $N(\tau)$ being as the distribution function with relaxation time τ. By taking short memory into account, the terms involving

$$\int_0^\infty \tau^n N(\tau)\mathrm{d}\tau, \quad n \geqslant 2, \tag{5}$$

are neglected in case of Walters' B fluid.[1] The velocity and temperature fields under the boundary layer approximations are governed by the following equations

$$\frac{\partial u}{\partial x} + \frac{\partial v}{\partial y} = 0, \tag{6}$$

$$u\frac{\partial u}{\partial x} + v\frac{\partial u}{\partial y} = \frac{\eta_0}{\rho}\left(\frac{\partial^2 u}{\partial y^2}\right) - \frac{k_0}{\rho}\left[u\frac{\partial^3 u}{\partial x \partial y^2} + v\frac{\partial^3 u}{\partial y^3} + \frac{\partial u}{\partial x}\frac{\partial^2 u}{\partial y^2} - \frac{\partial u}{\partial y}\frac{\partial^2 u}{\partial x \partial y}\right], \tag{7}$$

$$u\frac{\partial T}{\partial x} + v\frac{\partial T}{\partial y} = \sigma\frac{\partial^2 T}{\partial y^2} - \frac{\partial q_r}{\partial y} + q'', \tag{8}$$

$$u = u_{\mathrm{w}}(x) = ax, \quad v = v_{\mathrm{w}}, \quad -k\frac{\partial T}{\partial y} = h(T_{\mathrm{f}} - T) \ \text{ at } \ y = 0, \tag{9}$$

$$u \to 0, \quad T \to T_\infty \ \text{ as } \ y \to \infty, \tag{10}$$

where u and v represent the velocity components in the x and y directions, respectively, u_{w} is the velocity of the stretching sheet, v_{w} is the constant mass transfer velocity with $v_{\mathrm{w}} > 0$ for injection and $v_{\mathrm{w}} < 0$ for suction, T is the fluid temperature, T_∞ is the ambient fluid temperature, σ is the thermal diffusivity of the fluid, $\nu = (\mu/\rho)$ is the kinematic viscosity, and q'' is the non-uniform heat generated ($q'' > 0$) or absorbed ($q'' < 0$) per unit volume. For non-uniform heat source/sink, q'' is modeled by the following expression:

$$q'' = \frac{k u_{\mathrm{w}}(x)}{x\nu}\left[A(T_{\mathrm{s}} - T_\infty)f' + (T - T_\infty)B\right], \tag{11}$$

in which A and B are the coefficients of the space and the temperature-dependent heat source/sink, respectively, where prime denotes the differentiation with respect to η. Here two cases arise. For internal heat generation $A > 0$ and $B > 0$ and for internal heat absorption, we have $A < 0$ and $B < 0$, ρ is the density of the fluid, k is the thermal conductivity of fluid, T_{s} is the wall temperature, h is the convective heat transfer coefficient, and T_{f} is the convective fluid temperature below the moving sheet.

We define the similarity transformations as

$$\psi = x\sqrt{a\nu}f(\eta), \quad \theta(\eta) = \frac{T - T_\infty}{T_{\mathrm{f}} - T_\infty}, \ \eta = y\sqrt{\frac{a}{\nu}}, \tag{12}$$

where f is the dimensionless stream function, θ is the dimensionless temperature, and ψ is the stream function given by

$$u = \frac{\partial \psi}{\partial y}, \quad v = -\frac{\partial \psi}{\partial x}. \tag{13}$$

Now equation (6) is identically satisfied and equations (7)–(10) yield

$$f''' + ff'' - f'^2 + \beta(f''^2 - 2f'f'''' + ff'''') = 0, \tag{14}$$

$$\left(1 + \frac{4}{3}R\right)\theta'' + Pr\left(f\theta'\right) + Af' + B\theta = 0, \tag{15}$$

$$f = S, \quad f' = 1, \quad \theta' = -Bi[1 - \theta(0)] \quad \text{at } \eta = 0, \tag{16}$$

$$f' = 0, \quad \theta = 0 \quad \text{at } \eta = \infty, \tag{17}$$

where f', f'', f''', and f'''' are the derivatives of the stream function with respect to η, $\beta = k_0 a/\eta_0$ is the local Weissenberg number, $S = -v_{\mathrm{w}}/\sqrt{a\nu}$ is the mass transfer parameter with $S > 0$ for suction and $S < 0$ for injection, $Pr = \nu/\sigma$ is the Prandtl number, $R = (4\sigma^* T_\infty^3)/(kk^*)$ is the radiation parameter, and $Bi = (h/k)\sqrt{\nu/a}$ is the Biot number.

The skin friction coefficient C_{f} and local Nusselt number Nu_x are

$$C_{\mathrm{f}} = \frac{\tau_{\mathrm{w}}}{\frac{1}{2}\rho u_{\mathrm{w}}^2}, \quad Nu_x = \frac{x q_{\mathrm{w}}}{k(T_{\mathrm{f}} - T_\infty)}, \tag{18}$$

where the skin friction τ_{w} and the heat transfer from the plate q_{w} are

$$\tau_{\mathrm{w}} = \mu_0\left(\frac{\partial u}{\partial y}\right) + k_0\left\{u\frac{\partial^2 u}{\partial x \partial y} + 2\frac{\partial u}{\partial x}\frac{\partial u}{\partial y} + v\frac{\partial^2 u}{\partial y^2}\right\}\Big|_{y=0}, \tag{19}$$

$$q_{\rm w} = -k\frac{\partial T}{\partial y}\bigg|_{y=0} - \frac{16\sigma^* T_\infty^3}{3k^*}\frac{\partial T}{\partial y}\bigg|_{y=0}. \tag{20}$$

Dimensionless form of skin friction coefficient $C_{\rm f}$ and local Nusselt number Nu_x are

$$\begin{aligned} C_{\rm f}/Re_x^{1/2} &= (1-\beta)f''(0) - Sf'''(0),\\ Nu/Re_x^{1/2} &= -(1+\frac{4}{3}R)\theta'(0). \end{aligned} \tag{21}$$

In the above equation, $Re_x = \sqrt{\nu/xu_{\rm w}}$.

3. Homotopy analysis solutions

Initial approximations and auxiliary linear operators are chosen as

$$f_0(\eta) = S + (1 - {\rm e}^{-\eta}), \tag{22}$$

$$\theta_0(\eta) = \frac{Bi\exp(-\eta)}{1+Bi}, \tag{23}$$

$$\mathscr{L}_{\rm f} = f''' - f', \tag{24}$$

$$\mathscr{L}_\theta = \theta'' - \theta, \tag{25}$$

with properties

$$\mathscr{L}_{\rm f}(C_1 + C_2{\rm e}^{\eta} + C_3{\rm e}^{-\eta}) = 0, \tag{26}$$

$$\mathscr{L}_\theta(C_4{\rm e}^{\eta} + C_5{\rm e}^{-\eta}) = 0, \tag{27}$$

where C_i $(i = 1$–$5)$ are the arbitrary constants determined from the boundary conditions. If $p \in [0,1]$ denotes an embedding parameter, $h_{\rm f}$ and h_θ represent the non-zero auxiliary parameters then the zeroth order deformation problems are defined as

$$(1-p)\mathscr{L}_{\rm f}\left[\hat{f}(\eta;p) - f_0(\eta)\right] = ph_{\rm f}\mathscr{N}_{\rm f}\left[\hat{f}(\eta;p)\right], \tag{28}$$

$$\begin{aligned} &(1-p)\mathscr{L}_\theta\left[\hat{\theta}(\eta;p) - \theta_0(\eta)\right]\\ &\qquad = ph_\theta\mathscr{N}_\theta\left[\hat{f}(\eta;p), \hat{\theta}(\eta,p)\right], \end{aligned} \tag{29}$$

$$\begin{aligned} &\hat{f}(0;p) = S,\ \hat{f}'(0;p) = 1,\ \hat{f}'(\infty;p) = 0,\\ &\hat{\theta}'(0,p) = -Bi[1 - \theta(0,p)],\ \ \hat{\theta}(\infty,p) = 0, \end{aligned} \tag{30}$$

where $\mathscr{N}_{\rm f}$ and $\mathscr{N}_\theta$ are the nonlinear operators defined by

$$\begin{aligned} \mathscr{N}_{\rm f}[\hat{f}(\eta,p)] &= \frac{\partial^3\hat{f}(\eta,p)}{\partial\eta^3} + \hat{f}(\eta,p)\frac{\partial^2\hat{f}(\eta,p)}{\partial\eta^2} - \left(\frac{\partial\hat{f}(\eta,p)}{\partial\eta}\right)^2\\ &\quad + \beta\left[\left(\frac{\partial^2\hat{f}(\eta,p)}{\partial\eta^2}\right)^2 + \left(\hat{f}(\eta,p)\frac{\partial^4\hat{f}(\eta,p)}{\partial\eta^4}\right)\right.\\ &\quad \left. - 2\frac{\partial\hat{f}(\eta,p)}{\partial\eta}\frac{\partial^3\hat{f}(\eta,p)}{\partial\eta^3}\right], \end{aligned} \tag{31}$$

$$\begin{aligned} \mathscr{N}_\theta[\hat{\theta}(\eta,p), \hat{f}(\eta,p)] &= \left(1+\frac{4}{3}R\right)\frac{\partial^2\hat{\theta}(\eta,p)}{\partial\eta^2}\\ &\quad + Pr\left(\hat{f}(\eta,p)\frac{\partial\hat{\theta}(\eta,p)}{\partial\eta}\right)\\ &\quad + A\frac{\partial\hat{f}(\eta,p)}{\partial\eta} + B\hat{\theta}(\eta,p). \end{aligned} \tag{32}$$

When $p = 0$ and $p = 1$, then one has

$$\begin{aligned} &\hat{f}(\eta;0) = f_0(\eta),\ \hat{\theta}(\eta,0) = \theta_0(\eta) \text{ and } \hat{f}(\eta;1) = f(\eta),\\ &\hat{\theta}(\eta,1) = \theta(\eta), \end{aligned} \tag{33}$$

and when p variation is taken from 0 to 1, then $f(\eta,p)$ and $\theta(\eta,p)$ approach $f_0(\eta)$ and $\theta_0(\eta)$ to $f(\eta)$ and $\theta(\eta)$. Now f and θ in Taylor's series can be expanded as

$$f(\eta,p) = f_0(\eta) + \sum_{m=1}^{\infty} f_m(\eta)p^m, \tag{34}$$

$$\theta(\eta,p) = \theta_0(\eta) + \sum_{m=1}^{\infty} \theta_m(\eta)p^m, \tag{35}$$

$$\begin{aligned} f_m(\eta) &= \frac{1}{m!}\frac{\partial^m f(\eta;p)}{\partial\eta^m}\bigg|_{p=0},\\ \theta_m(\eta) &= \frac{1}{m!}\frac{\partial^m\theta(\eta;p)}{\partial\eta^m}\bigg|_{p=0}, \end{aligned} \tag{36}$$

where the convergence depends on $h_{\rm f}$ and h_θ. By appropriately choosing $h_{\rm f}$ and h_θ, the series (34) and (35) converge for $p = 1$ and so

$$f(\eta) = f_0(\eta) + \sum_{m=1}^{\infty} f_m(\eta), \tag{37}$$

$$\theta(\eta) = \theta_0(\eta) + \sum_{m=1}^{\infty} \theta_m(\eta). \tag{38}$$

The m-th order deformation problems can be provided as

$$\mathscr{L}_{\rm f}[f_m(\eta) - \chi_m f_{m-1}(\eta)] = h_{\rm f}\mathscr{R}_{\rm f}^m(\eta), \tag{39}$$

$$\mathscr{L}_\theta[\theta_m(\eta) - \chi_m\theta_{m-1}(\eta)] = h_\theta\mathscr{R}_\theta^m(\eta), \tag{40}$$

$$\begin{aligned} &f_m(0) = f_m'(0) = f_m'(\infty) = 0,\\ &\theta_m'(0) - Bi\theta_m(0) = \theta_m(\infty) = 0, \end{aligned} \tag{41}$$

$$\begin{aligned} \mathscr{R}_{\rm f}^m(\eta) &= f_{m-1}'''(\eta) + \sum_{k=0}^{m-1}\left[f_{m-1-k}f_k'' - f_{m-1-k}'f_k'\right]\\ &\quad + \beta\sum_{k=0}^{m-1}(f_{m-1-k}''f_k'' + f_{m-1-k}f_k'''' - 2f_{m-1-k}'f_k'''), \end{aligned} \tag{42}$$

$$\begin{aligned} \mathscr{R}_\theta^m(\eta) &= \left(1+\frac{4}{3}R\right)\theta_{m-1}'' + Pr\sum_{k=0}^{m-1}\theta_{m-1-k}'f_k\\ &\quad + Af_{m-1}' + B\theta_{m-1}, \end{aligned} \tag{43}$$

$$\chi_m = \begin{cases} 0, & m \le 1,\\ 1, & m > 1. \end{cases} \tag{44}$$

The general solutions of Eqs. (39)–(41) can be expressed by the following equations

$$f_m(\eta) = f_m^*(\eta) + C_1 + C_2{\rm e}^{\eta} + C_3{\rm e}^{-\eta}, \tag{45}$$

$$\theta_m(\eta) = \theta_m^*(\eta) + C_4{\rm e}^{\eta} + C_5{\rm e}^{-\eta}, \tag{46}$$

where f_m^* and θ_m^* are the particular solutions of Eqs. (39) and (40) and constants C_i $(i = 1$–$5)$ can be determined by the boundary conditions (41). They are given by

$$C_2 = C_4 = 0,\ C_3 = \frac{\partial f^*(\eta)}{\partial\eta}\bigg|_{\eta=0},\ C_1 = -C_3 - f^*(0), \tag{47}$$

$$C_5 = \frac{1}{Bi+1}\left[\left.\frac{\partial\theta^*(\eta)}{\partial\eta}\right|_{\eta=0} - Bi\theta^*(0)\right]. \quad (48)$$

4. Convergence of the homotopy solutions

Series (37) and (38) have nonzero auxiliary parameters $\hbar_f$ and $\hbar_\theta$ that help us to control and adjust the convergence of series solutions. For admissible values of $\hbar_f$ and $\hbar_\theta$, we plotted the $\hbar$ curves of $f''(0)$ and $\theta'(0)$. Figures 1 and 2 show that the ranges of admissible values of $\hbar_f$ and $\hbar_\theta$ are $-1.8 \le \hbar_f \le -0.3$ and $-1.9 \le \hbar_\theta \le -0.55$ respectively. The series converge in the whole region of η when $\hbar_f = -1.5$ and $\hbar_\theta = -1.3$. Table 1 displays the convergence of homotopy solution for different orders of approximations.

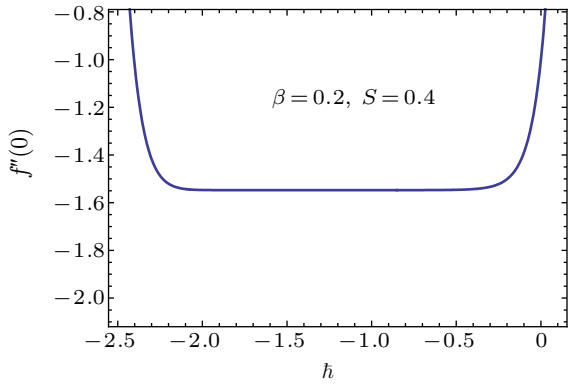


Fig. 1. (color online) $\hbar$ curve for velocity field.

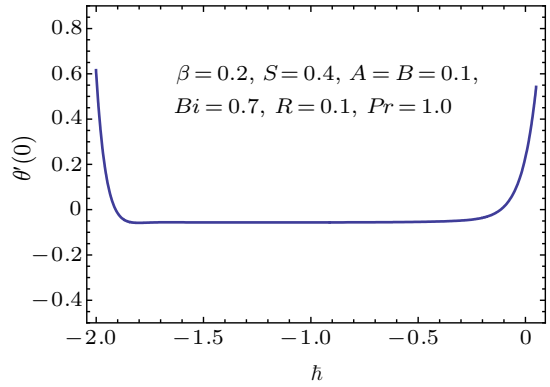


Fig. 2. (color online) $\hbar$ curve for temperature field.

Table 1. Convergence of HAM solution for different orders of approximations when $S = 0.4$, $\beta = 0.2$, $A = B = 0.1$, $Pr = 1$, $Bi = 0.7$, and $R = 0.1$.

Order of approximation	$-f''(0)$	$-\theta'(0)$
1	1.51000	0.047359
5	1.54617	0.027114
10	1.54727	0.030756
15	1.54728	0.031432
20	1.54728	0.031568
25	1.54728	0.031601
30	1.54728	0.031608
35	1.54728	0.031611
40	1.54728	0.031611
50	1.54728	0.031611

5. Results and discussion

Here we focus on the behaviors of different physical parameters entering into the series solutions. In particular, the plots for the dimensionless velocity gradient and heat transfer rate at the bounding surface are displayed and discussed. Here the velocity decreases with the increase of β, which corresponds to a thinner momentum boundary layer. The viscoelasticity produces tensile stress, which contracts the boundary layer and consequently the velocity decreases (see Fig. 3). An increase in the suction parameter moves the velocity distribution towards the boundary, indicating a decrease in the thickness of the boundary layer (see Fig. 4). It is worth mentioning here that the porous stretching sheet of this type with suction beneath it is sometimes used to prevent the boundary layer from separating.

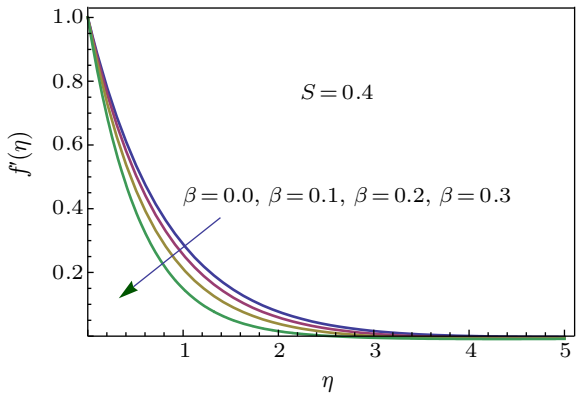


Fig. 3. (color online) Influence of β on $f'(\eta)$.

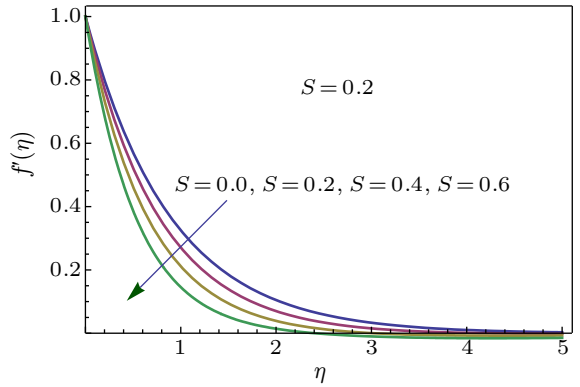


Fig. 4. (color online) Influence of S on $f'(\eta)$.

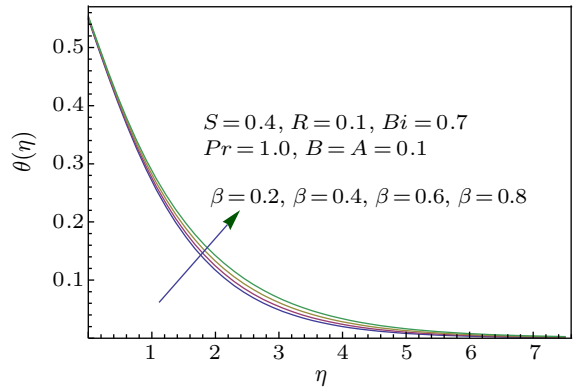


Fig. 5. (color online) Influence of β on $\theta(\eta)$.

Figure 5 shows the influence of viscoelastic parameter β on temperature. We found that the temperature and the thermal boundary layer thickness decrease as the viscoelastic effects strengthen. The influence of Biot number Bi is shown in Fig. 6. As expected, an increase in Bi results in a stronger convective heating, which increases the surface temperature. This allows the thermal effect to penetrate more deeply into the quiescent fluid. The outcome is consistent with the findings reported by Aziz.[11] The variation of temperature distribution with the Prandtl number Pr is presented in Fig. 7. From the physical point of view, the larger Prandtl number coincides with the weaker thermal diffusivity and thinner boundary layer. This is because a higher Prandtl number fluid has a relatively low thermal conductivity, which reduces conduction and thereby increases the variations of thermal characteristics. Figure 8 shows that temperature θ appreciably rises when the thermal radiation effect is strengthened. However, suction reduces the thermal boundary layer thickness, as can be seen from Fig. 9. Figures 10 and 11 show the influences of the heat source/sink parameters on temperature θ. As expected, the larger heat source parameter enhances the temperature distribution to a great extent and thus largely contributes to the growth of a thermal boundary layer. Also energy is absorbed for reducing values of $A < 0$ and $B < 0$ and this causes the magnitude of the temperature to decrease, whereas non-uniform heat sink corresponding to $A < 0$ and $B < 0$ can contribute to quenching the heat from the stretching sheet effectively.

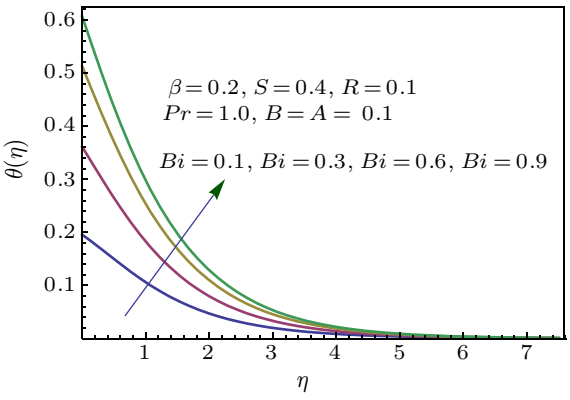


Fig. 6. (color online) Influence of Bi on $\theta(\eta)$.

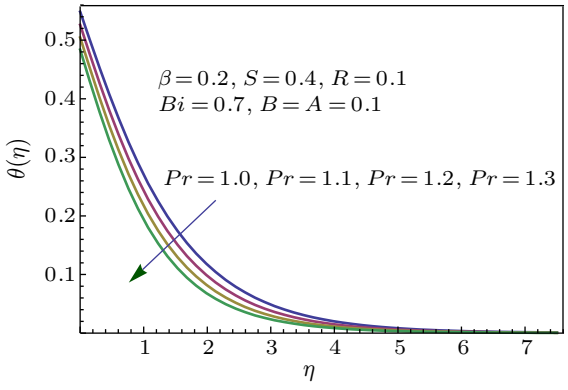


Fig. 7. (color online) Influence of Pr on $\theta(\eta)$.

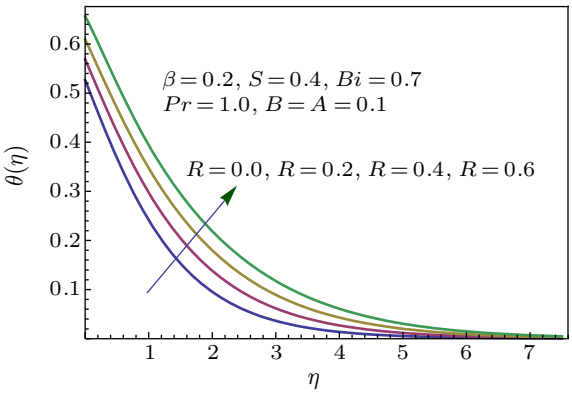


Fig. 8. (color online) Influence of R on $\theta(\eta)$.

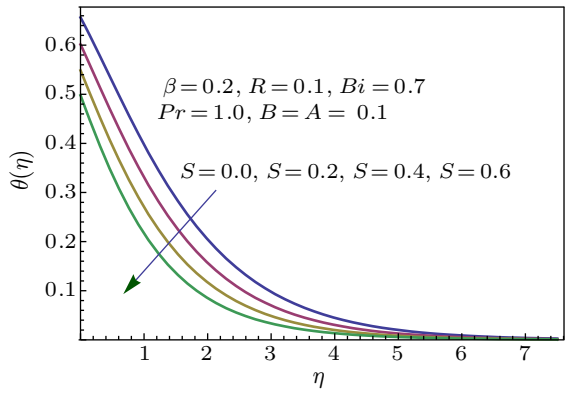


Fig. 9. (color online) Influence of S on $\theta(\eta)$.

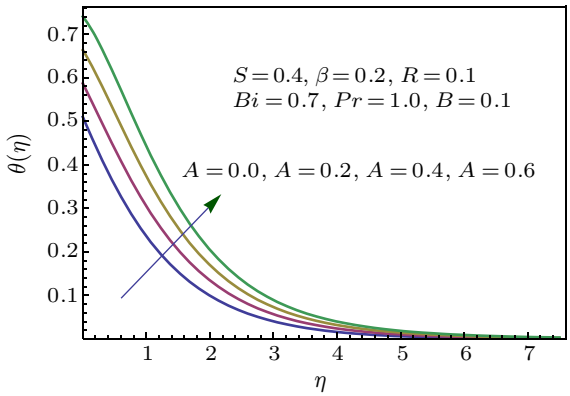


Fig. 10. (color online) Influence of A on $\theta(\eta)$.

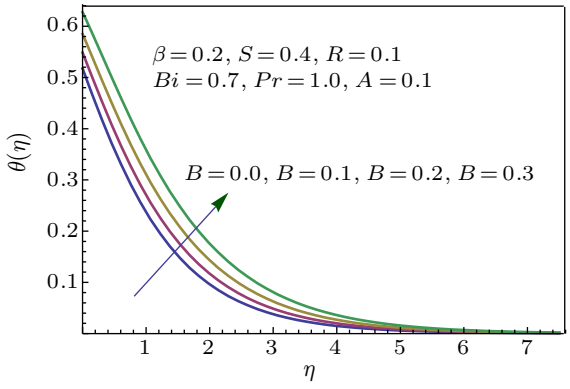


Fig. 11. (color online) Influence of B on $\theta(\eta)$.

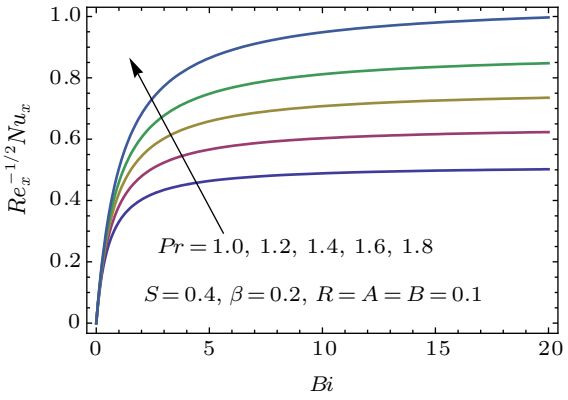


Fig. 12. (color online) Influence of $Re_x^{-1/2}Nu_x$ on Pr with $S = 0.4$, $\beta = 0.2$, $R = A = B = 0.1$.

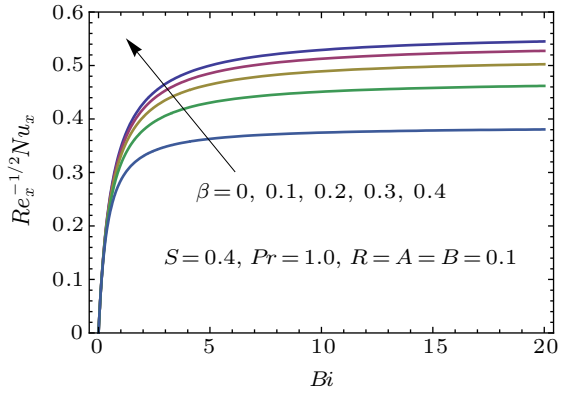


Fig. 13. (color online) Influence of $Re_x^{-1/2}Nu_x$ on β with $S = 0.4$, $Pr = 1.0$, $R = A = B = 0.1$.

Table 2. Values of skin friction coefficient $Re_x^{1/2}C_f$ for the parameters S and β.

S	β	$-Re_x^{1/2}C_f$
0.0	0.2	0.870726
0.2		0.849053
0.4		0.712725
0.6		0.364968
	0.0	1.2198
	0.1	1.01937
	0.2	0.712725

Table 2 provides the numerical values of the dimensionless velocity gradient at the wall for different values of suction parameter S and viscoelastic parameter β. It is clear that increases of S and β reduce the dimensionless velocity gradient on the stretching surface. This is a very useful result from the industrial point of view, since the power generation involved in displacing the fluid over the sheet is reduced by assuming sufficiently large values of these parameters. The numerical values of the local Nusselt number for different values of embedded parameters have been tabulated (see Table 3). It is already indicated that larger convective heating at the bounding surface generates larger heat flux from the surface, which eventually increases the magnitude of the local Nusselt number. It is clear from Fig. 4 that although the thermal boundary layer thins but profiles become increasingly steeper with the increase of the value of Pr. The Nusselt number, being proportional to the increase of the initial slope with the augment of the value of Pr. On the other hand, the magnitude of the local Nusselt number decreases as the viscoelastic effect strengthens.

Table 3. Values of local Nusselt number $Nu/Re_x^{1/2}$ for the parameters Bi, R, Pr, S, and β.

Bi	Pr	β	S	R	$Nu/Re_x^{1/2}$
0.4	1.0	0.2	0.4	0.1	0.223253
0.6					0.280333
0.8					0.321423
0.7	1.1				0.323167
	1.2				0.340928
	1.3				0.356453
		0.0			0.313797
		0.1			0.309528
		0.2			0.302425
			0.2		0.257777
			0.3		0.281064
			0.5		0.321888
				0.0	0.322187
				0.1	0.302425
				0.2	0.284298

6. Summary

Boundary layer flow of Walters' B fluid over a porous stretching sheet with radiation and non-uniform heat source/sink is investigated here. The series solutions of the governing mathematical problems are obtained by using HAM and appropriately choosing the convergence control parameters. Thus the convergent solutions are obtained through plots of $\hbar$ curves. It is noticed that velocity and wall shear stress decrease with the increase of viscoelastic parameter β whereas temperature θ is an increasing function of β. An increase in the suction parameter S also reduces the momentum boundary layer. The temperature θ and rate of heat transfer at the sheet increase with the increase of convective heating at the sheet surface. For sufficiently large values of Biot number Bi, the results for the case of constant wall temperature $(\theta(0) = 1)$ can be recovered. Moreover, the present finding for the Newtonian fluid case can be retrieved by choosing $\beta = 0$.

References

[1] Beard W D and Walters K 1964 *Proc. Camb. Philos. Soc.* **60** 667
[2] Soundalgekar M V 1978 *Czechoslovak J. Phys. B* **28** 1217
[3] Samria K N, Reddy S U M and Prasad R 1990 *Astrophys. Space Sci.* **172** 231
[4] Rajagopal K R, Na T Y and Gupta A S 1984 *Rheo. Acta* **23** 213
[5] Labropulu F, Hussain I and Chinichian M 2004 *Int. J. Math. Sci.* **2004** 3249
[6] Khan K S and Sanjayanand E 2005 *Int. J. Heat Mass Transfer* **48** 1534
[7] Cortell R 2007 *Chem. Eng. Process.* **46** 982
[8] Abel S M, Sanjayanand E and Nandeppanavar M M 2008 *Commun. Nonlinear Sci. Numer. Simul.* **13** 1808
[9] Hayat T, Sajid M and Pop I 2008 *Nonlinear Analysis: RWA* **9** 1811
[10] Hayat T, Mustafa M and Sajid M 2011 *Numer. Meth. Part. Diff. Eq.* **27** 915
[11] Fakhar K, Xu Z L and Cheng Y 2007 *Chin. Phys. Lett.* **24** 1129

[12] Hayat T, Mustafa S and Obaidat M 2011 *Chin. Phys. Lett.* **28** 074702
[13] Ali N, Sajid M, Javad T and Abbas Z 2011 *Chin. Phys. Lett.* **28** 014704
[14] Hayat T, Abbasi F M and Hendi A A 2011 *Chin. Phys. Lett.* **28** 044701
[15] Hayat T, Saleem N and Hendi A A 2011 *Chin. Phys. Lett.* **28** 034702
[16] Yuan M J, Yu B M, Zhang W and Yuan J 2011 *Acta Phys. Sin.* **60** 024703 (in Chinese)
[17] Sajid M, Mahmood K and Abbas Z 2012 *Chin. Phys. Lett.* **29** 024702
[18] Bhattacharyya K, Hayat T and Alsaedi A 2013 *Chin. Phys. B* **22** 024702
[19] Aziz A 2009 *Commun. Nonlinear Sci. Numer. Simul.* **14** 1064
[20] Magyari E 2011 *Commun. Nonlinear Sci. Numer. Simul.* **16** 599
[21] Hayat T, Shehzad S A, Alsaedi A and Alhothuali S M 2012 *Chin. Phys. Lett.* **29** 114704
[22] Ishak A 2010 *Appl. Math. Comput.* **217** 837
[23] Yao S, Fang T and Zhong Y 2011 *Commun. Nonlinear Sci. Numer. Simul.* **16** 752
[24] Hayat T, Asad S, Qasim M and Hendi A A 2012 *Int. J. Numer. Meth. Fluids* **69** 1350
[25] Hayat T, Shehzad A S, Qasim M and Obaidat S 2011 *Therm. Sci.* **15** 253
[26] Mustafa M, Hayat T and Alsaedi A 2012 *Curr. Nanosci.* **8** 328
[27] Wang J F and Cheng Y M 2012 *Chin. Phys. B* **21** 120206
[28] Chen L, Ma H P and Cheng Y M 2013 *Chin. Phys. B* **22** 050202
[29] Zhang Z, Wang J F, Cheng Y M and Liew K M 2013 *Sci. China: Phys. Mech. Astron.* **56** 1568
[30] Liao J S 2009 *Commun. Nonlinear Sci. Numer. Simul.* **14** 983
[31] Nadeem S and Faraz N 2010 *Chin. Phys. Lett.* **27** 034704
[32] Abbasbandy S 2008 *Z. Angew. Math. Phys.* **59** 51
[33] Rashidi M M and Pour M A S 2010 *Nonlinear Analysis: Modelling and Control* **15** 83
[34] Rashidi M M, Hayat T, Erfani Pour M E S A and Hendi A A 2011 *Commun. Nonlinear Sci. Numer. Simul.* **16** 4303
[35] Hayat T and Qasim M 2010 *Commun. Nonlinear Sci. Numer. Simul.* **15** 2375
[36] Hayat T, Mustafa M and Obaidat S 2011 *Chin. Phys. Lett.* **28** 074702
[37] Hayat T, Mustafa M and Asghar S 2010 *Nonlinear Analysis: RWA* **11** 3186
[38] Hayat T, Naz R and Sajid M 2010 *Commun. Nonlinear Sci. Numer. Simul.* **15** 581
[39] Akbar S N and Nadeem S 2013 *Chin. Phys. Lett.* **27** 034704